

State filling and time-resolved photoluminescence of excited states in $\text{In}_x\text{Ga}_{1-x}\text{As}/\text{GaAs}$ self-assembled quantum dots

S. Raymond,^{*} S. Fafard, P. J. Poole, A. Wojs,[†] P. Hawrylak, and S. Charbonneau
Institute for Microstructural Sciences, National Research Council, Ottawa, Ontario, Canada K1A 0R6

D. Leonard, R. Leon,[‡] P. M. Petroff, and J. L. Merz[§]
*Center for Quantized Electronic Structures (QUEST) and Materials Department and Electrical and Computer Engineering Department,
University of California at Santa Barbara, Santa Barbara, California 93106*

(Received 31 July 1995; revised manuscript received 25 April 1996)

We present radiative lifetime measurements of excited states in semiconductor self-assembled quantum dots. By increasing the photoexcitation intensity, excited-state interband transitions up to $n=5$ can be observed in photoluminescence. The dynamics of the interband transitions and the intersublevel relaxation in these zero-dimensional energy levels lead to state filling of the lower-energy states, allowing the Fermi level to be raised by more than 200 meV due to the combined large intersublevel spacing and the low density of states. The decay time of each energy level obtained under various excitation conditions is used to evaluate the intersublevel thermalization time. [S0163-1829(96)06839-7]

The dynamics of carriers confined in semiconductor quantum structures with allowed momentum in at least one direction leads to rapid thermalization with the lattice, and consequently radiative recombination originating predominantly from the lowest available state(s). For quantum dots (QD's) however, the zero-dimensional (0D) discrete density of states imposes more severe thermalization rules,^{1,2} which can translate to the observation of photoluminescence (PL) from excited-state transitions at low excitation intensities due to the restricted intersublevel relaxation rates.³ Due to this *phonon bottleneck* effect, efficient carrier relaxation toward the ground states occur predominantly between levels which are separated by not more than a few meV using longitudinal-acoustic (LA)-phonon emission, or by an energy within a few meV from the longitudinal-optic (LO) phonon energies.⁴⁻⁶ However, it has been shown that thermalization can also be achieved efficiently due to multiphonon processes^{5,7} or Coulomb interactions.⁸ For example, the inhomogeneously broadened Gaussian PL line shape originating from the statistically distributed ground states of small self-assembled QD's obtained using spontaneous island formation⁹⁻¹⁵ indicates that the intersublevel relaxation rates are much faster than the ~ 1 -ns interband dynamics of the ground states.¹⁶ Furthermore, the atomiclike discrete energy spectrum of each QD state is expected to lead to a *state-filling* effect due to exclusion principles taking effect when only a few carriers populate the lower states. This will also lead to hindered intersublevel dynamics, and to the observation of excited-state interband transitions as the excitation intensity is increased. This has also been observed experimentally with larger self-assembled QD's,^{4,17} which support a greater number of excited states,¹⁸ with hole levels in small pyramidal self-assembled QD's,¹⁹ and with QD's created by potential deformation in a quantum well (QW) stressed with self-assembled QD's.²⁰ The phonon bottleneck and the state-filling effects both lead to emission peaks at higher energy than the ground-state emission, but should not be confused with the higher-energy emission commonly observed in the

case of ML fluctuations in a QW. Indeed the excitons localized in the potential fluctuation of a QW can be used to produce natural QD's.²¹⁻²³ PL microspectroscopy of these natural QD's reveals a very sharp homogeneous linewidth of the ground-state emission similar to the one observed with self-assembled QD's,^{10,11,7} and excitation spectroscopy has also been used to reveal excited states which have an energy splitting comparable to the QW inhomogeneous broadening. Also, in the absence of strain-induced self-assembling processes,^{24,25} monolayer fluctuations can lead to *segregated inhomogeneous broadening*, resulting in multiplex PL emission when observed in macrospectroscopy. For example Marquezini *et al.* recently reported PL emission of thin InAs/InP QW's displaying up to five peaks, corresponding to the ground-state PL emission in QW's having a local thickness of 1-5 ML, respectively.²⁶

The above three effects (phonon bottleneck, state filling, and segregated inhomogeneous broadening) can give rise to higher-energy emission peak(s), but possess characteristic features specific to the different physics involved in each. For example, the state-filling effect is the only one which will show clear saturation effects. At low intensity only the (inhomogeneously broadened) ground-state levels are observed because of the fast intersublevel relaxation in the case of bare levels with no significant phonon bottleneck effect. As the intensity is increased, a progressive saturation of the lower-energy transitions is combined with the emergence of emission peaks originating from the excited-state interband radiative transitions. These are observed as intersublevel carrier relaxation toward the lower level is slowed due to the reduced number of available final states.^{4,17,19,20} In contrast, the phonon bottleneck effect will permit excited-state interband transitions even in low excitation conditions because the intersublevel and interband relaxation dynamics are comparable.³ On the other hand, the multiple peaks observed in the case of segregated inhomogeneous broadening are usually observed with the same relative amplitude over several orders of magnitude of excitation intensity, since they

reflect the relative abundance of a given ground-state energy relative to the other available ground-state energies in the probed area.²⁶ Consequently, the energy position of the peaks observed in the case of segregated inhomogeneous broadening in QW's follow the energy predicted for a QW with a fluctuation of a few ML from its mean deposited thickness. In contrast, in self-assembled QD's the energy spectra of the excited states are typically quite different from the ML fluctuation energies due to the lateral confinement. Also, contrary to the other two cases, the higher-energy peaks observed in the case of the segregated inhomogeneous broadening all originate from ground-state transitions which will behave very differently under an external perturbation. For example, in a magnetic field the ground states will exhibit normal diamagnetic shifts, whereas the excited states will show more complex splitting with shifts to lower energies and with restoration of the dynamical symmetry at some specific fields.^{18,27-29} For the case of excitons localized in natural dots in thin QW's with ML fluctuations, they are confined by a much shallower potential than in the case of self-assembled QD's obtained by the spontaneous island formation, and are therefore easily distinguished when the available thermal energy is increased.^{30,31} The onset of thermionic emission and the thermal PL quenching is therefore observed at much higher temperatures in self-assembled QD's due to their deeper confining potentials.

In virtue of their relatively rapid intersublevel dynamics and well-defined 0D density of states, larger self-assembled QD's, which can accommodate several excited states with an electronic intersublevel spacing comparable to the LO-phonon energy, represent an ideal quantum system to study state-filling effects. For example, the observed PL peak separation between the radiative recombination of adjacent excited states in self-assembled QD's 36.5 nm in diameter is ~ 50 meV.⁴ This allows the excited-state transitions to be resolved from the Gaussian inhomogeneous broadening which for self-assembled QD's typically yield a full width at half maximum (FWHM) of ~ 50 meV. This broadening arises from small fluctuations in the QD's confining size, the alloy composition variations, and the shifts due to strain-field effects. The major contribution to the inhomogeneous broadening comes from the size variation due to the large confining potentials and the small volumes. However, due to self-organizing processes, segregated inhomogeneous size broadening is not normally observed in $\text{In}_x\text{Ga}_{1-x}\text{As}/\text{GaAs}$ self-assembled QD's. Under favorable growth conditions, the alloy fluctuations can be minimized, and would certainly never lead to segregated inhomogeneous alloy broadening under normal conditions. Finally, although the total-energy shifts due to strain fields are more than 100 meV,³² the QD to QD variations are again small due to the self-organization of the strain fields, leading to a normal distribution of the next-neighbor distances^{24,25} which also prevents the possibility of segregated inhomogeneous strain-field broadening. In addition, many-body phenomena such as biexcitons, charge excitons, exciton complexes, and band-gap renormalization can also contribute to the broadening at higher excitation intensities, but for a large ensemble of QD's they will be difficult to resolve from the above inhomogeneous broadening mechanisms, as they can only shift the emission energy by few meV.^{33,18} It is therefore the purpose of this paper to

analyze the dynamics of excited states in such self-assembled QD's with well-defined excited-state spectra, and study the influence of the state filling on the intersublevel thermalization and the interband radiative recombination.

The self-assembled QD's used for the present study exhibit state filling with up to four observable excited state interband transitions.⁴ The sample has been grown by molecular-beam epitaxy using the Stranski-Krastanow growth mode. The sample structure grown on a GaAs(100) substrate consists of a 500 nm GaAs buffer layer, followed by the QD layer where 6.5 ML of $\text{In}_{0.5}\text{Ga}_{0.5}\text{As}$ were grown at a nominal temperature of 530 °C, and covered with a 30-nm GaAs cap layer. The PL measurements were performed at 4 K using for the excitation source either a steady-state (cw) Ar^+ , or a YAG (yttrium aluminum garnet) pumped rhodamine 640 dye laser system providing 5-ps pulses at 630.0 nm at a repetition rate of 76 MHz. The beam was focused to a spot ~ 80 μm in diameter at the sample surface, thus probing a population of $\sim 5 \times 10^5$ dots. The luminescence was dispersed by a 0.64-m spectrometer, and either detected, with a cooled germanium detector using synchronous detection techniques for the cw measurements, or collected and analyzed via an up-conversion technique using a LiIO_3 crystal for time-resolved PL (TRPL) measurements.³⁴ This TRPL system provided a temporal resolution of ~ 10 ps.

Transmission electron microscopy (TEM) was performed on a piece adjacent³⁵ to the sample studied optically to insure that the self-assembling growth proceeded normally, and that no segregated inhomogeneous size or strain-field broadening can be present in the PL spectra due to monolayer fluctuations or gross size or distribution nonuniformities. As can be inferred from the picture, the dot density is 100 μm^{-2} , and their average diameter is 36.5 nm, which yields a coverage of 10%. Note that the inset shows that the QD size uniformity is better than 10%. Figures 2(a) and 2(b) show the cw PL spectra obtained for different excitation intensities. At very low excitation density (0.050 W/cm²), only one emission peak is observed at 1.10 eV with a shoulder at 1.13 eV. As the power is increased, five peaks are resolved, including the ground state.⁴ These peaks are separated by ~ 40 meV (in the case of the highest excited states) and ~ 50 meV (in the case of the lowest states). Their FWHM ranges from 30 to 40 meV, as deduced from a multiple Gaussian fit. Figure 2(c) shows the time-integrated spectra obtained for pulsed excitation. Also, for comparison, the calculated emission energies for a corresponding hypothetical QW with a various number of ML is shown at the top of Fig. 2. From the good QD size and near-neighbor distance uniformities observed in Fig. 1, and from the complete lack of correlation of the emission energies with the emission expected for ML fluctuations, the possibility of segregated inhomogeneous broadening can be unambiguously ruled out.³⁶ Furthermore, the emission peaks observed in Fig. 2 have the temperature dependence expected for excitons localized in deep confining potentials.³¹ Here some radiative recombination can still be observed at room temperature, whereas excitons localized in shallow minima grossly suffering from segregated inhomogeneous broadening would be quenched at much lower temperatures depending on the localization potential [typically a few tens of K (Ref. 30)]. Finally, the excited-state nature of these

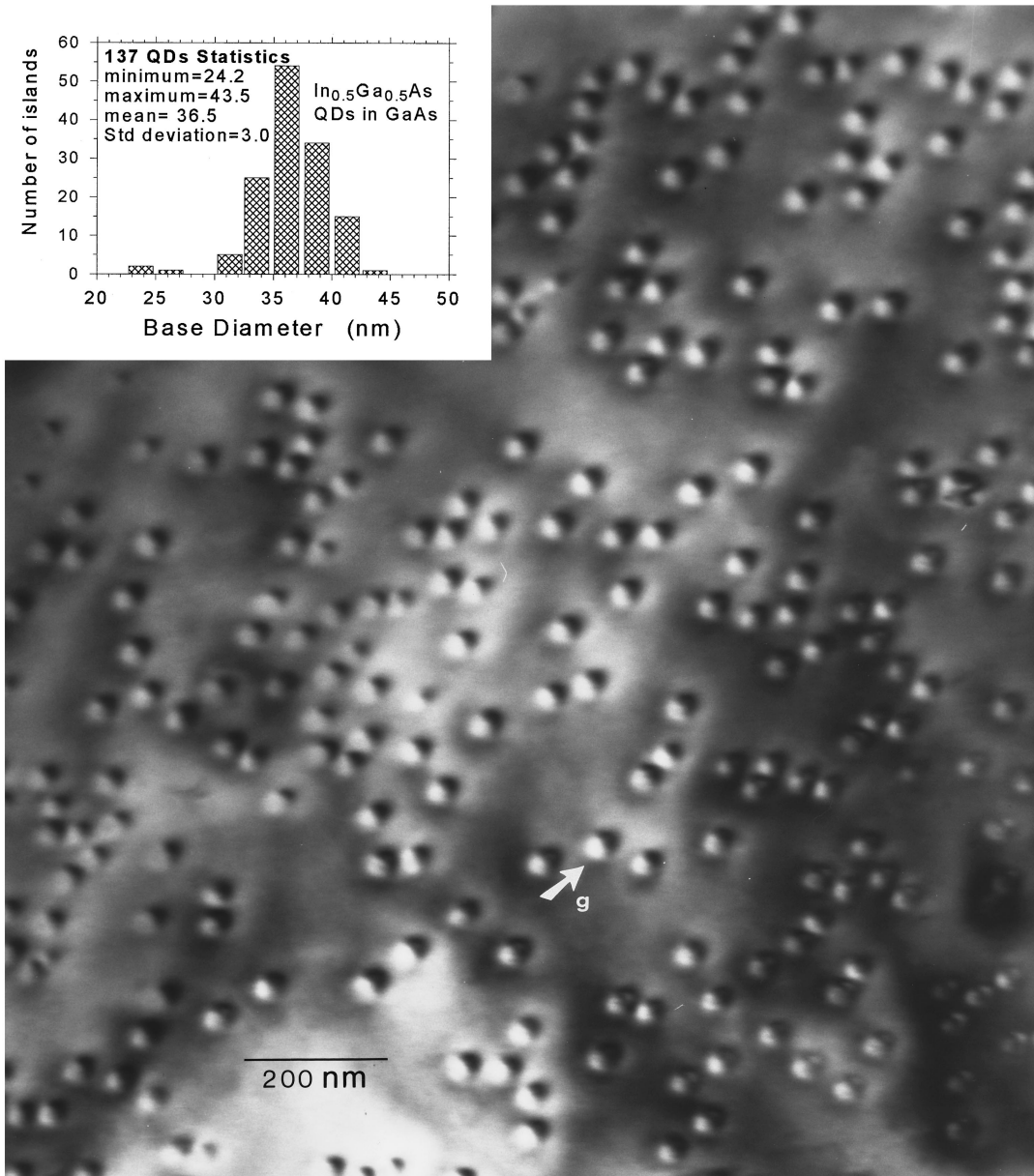


FIG. 1. Dark-field TEM plan view micrograph of the $\text{In}_x\text{Ga}_{1-x}\text{As}/\text{GaAs}$ sample. The dark-light contrast seen is obtained under two beam dynamical diffraction conditions. The operating diffraction vector is always perpendicular to the dark-light lobes, indicating a radially symmetric strain field. The inset shows some statistics obtained from the TEM picture.

higher-energy transitions has recently been confirmed beyond any possible doubt by measuring the magnetic-field dependence of the observed peaks.²⁹

The expected electronic levels of the QD's were calculated with the structural information provided by the growth, the TEM, and the PL results. The QD is modeled as a hemispherical cap,²⁵ with a fixed height h and a radius at the base s , formed on a wetting layer (WL) of thickness t_w . The confining potential V_c is zero inside the dot and the wetting layer, and finite outside. The effective-mass Hamiltonian, and the adiabatic approximation are used to describe the conduction- and valence-band states in the QD. Our model includes electron-hole Coulomb interaction, and the influence of strain was also partially considered. The precise strain distribution in these dots is still a matter of discussion,³² so in a first approximation we used the strain

distribution typical of a QW system with the same composition. In the adiabatic approximation, we first find the energy $E(\rho)$ corresponding to the motion along the growth direction for a given thickness of the dot at the radial coordinate ρ . The radial motion for each angular momentum channel in the effective confining potential $E(\rho)$ is next solved exactly. In order to carry those calculations, the average QD height is first estimated by computing the thickness of a QW that would emit at the same ground-state energy than the QD's. The total QD thickness thus obtained is 6.0 nm. Next, from the QD coverage, the average volume, and the total amount of material deposited, the WL thickness is estimated to be 1.6 nm. Results are presented in Fig. 3. The solid bars indicate the energy levels of a single QD with $s=18$ nm, $h=4.4$ nm, and $t_w=1.6$ nm, while the dashed line shows the absorption spectrum $D(\omega)$ of an ensemble of dots, with a size dis-

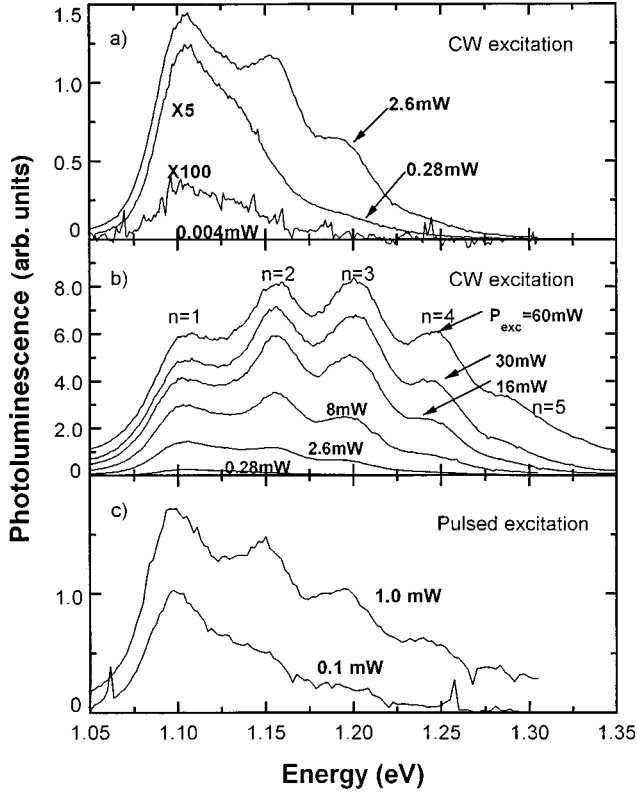


FIG. 2. Low-temperature (4 K) PL spectra of $\text{In}_{0.5}\text{Ga}_{0.5}\text{As}/\text{GaAs}$ self-assembled QD's 36.5 nm in diameter, displaying excited-state radiative recombination as the intensity is increased. Spectra excited with a cw Ar-ion laser at different excitation intensities in (a) and (b), and excited at 1.968 eV with a pulsed dye laser in (c). With pulsed excitations, the excited-state emission is obtained at slightly lower excitation intensities. To illustrate that the PL arises from the excited states and not from ML fluctuations in a QW, the calculated emission energies for a corresponding hypothetical QW with a various number of ML is shown with the vertical bars at the top of figure.

tribution consistent with what is found in Fig. 1. If we are to assume the nonequilibrium distribution function $n(\omega) = e^{-\beta\omega}$, the emission spectrum of a highly excited group of QD's is given by $E(\omega) = n(\omega)D(\omega)$, as shown in Fig. 3 (solid line). It is found that there are indeed five groups of bound states below the confined states of the wetting layer. These groups correspond to states with different angular momenta m . Their grouping and spacing is consistent with a shell structure of a QD with an effective parabolic confining potential. The line shape of the spectrum and the relative position of the peaks qualitatively correspond to experimental results. This simple calculation shows that good agreement can be obtained between experiment and theory using an ensemble of self-assembled QD's with excited-state emission. Observed discrepancies may come from differences in the real versus the assumed QD shape. The effects of exciton-exciton interactions have also been neglected. In particular, it is expected that the ground-state emission is significantly broadened by biexcitonic recombinations.

Time-resolved spectroscopy was used to monitor the time evolution of each emission line observed, and obtain information on the dynamics of the interband radiative recombi-

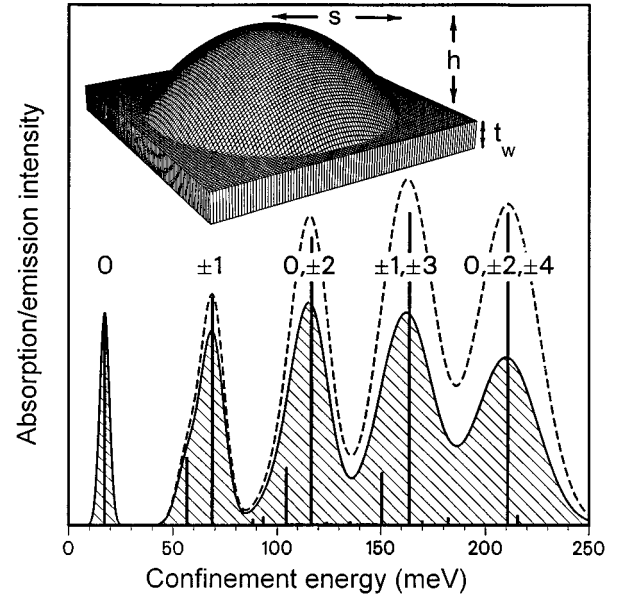


FIG. 3. Absorption spectrum (dashed line) and emission spectrum (solid line) obtained from theoretical calculations for an ensemble containing many dots. The bars indicate the position of the energy levels for a single dot with a potential profile, as shown in the inset. The amplitude of the bars is proportional to their oscillator strengths. The parameter values are $s=18$ nm, $h=4.4$ nm, and $t_w=1.6$ nm. The numbers indicate the allowed angular momenta which are consistent with the dot symmetry.

nation and the intersublevel thermalization. The time-dependent trace for each PL peak is shown in Fig. 4 for an average excitation intensity of 13 W/cm^2 . The decay part of each curve was empirically fitted to a single exponential function of the form $Ae^{-t/\tau}$ in order to extract a decay time constant. The ground state as well as the first and second excited states do not seem to show a single exponential decay due to the state-filling effect, but, for the dynamic range permitted by the experiment, deviations from the trial function were small. The same procedure was applied for two other excitation intensities, namely, 1.3 and 325 W/cm^2 , and Table I summarizes the results obtained. The results presented in Fig. 2 and Table I can be summarized as follows: excited-state emission and absolute saturation of the amplitude of the lower transitions are observed as the excitation intensity is increased; the decay time of a given transition increases with the excitation intensity to finally saturate slightly above 1 ns; and, finally, the upper transitions have faster decay times. The above observations are all consistent with state filling effects in QD's as described above.

Let us first discuss the cw PL experiment. The carriers are first created in the barrier material (GaAs), and those created in the vicinity of the QD layer will be captured by the QD's. Precise information about the capture process is not available at the moment, but carriers should first fall in the 2D continuum states of the WL before being trapped by a QD. Without more precise experimental evidence, one has to consider that the carriers can then possibly fall directly into any of the available discrete bound states, with no need to occupy all the excited states sequentially. However, since more states are available in higher-energy levels, most carriers will

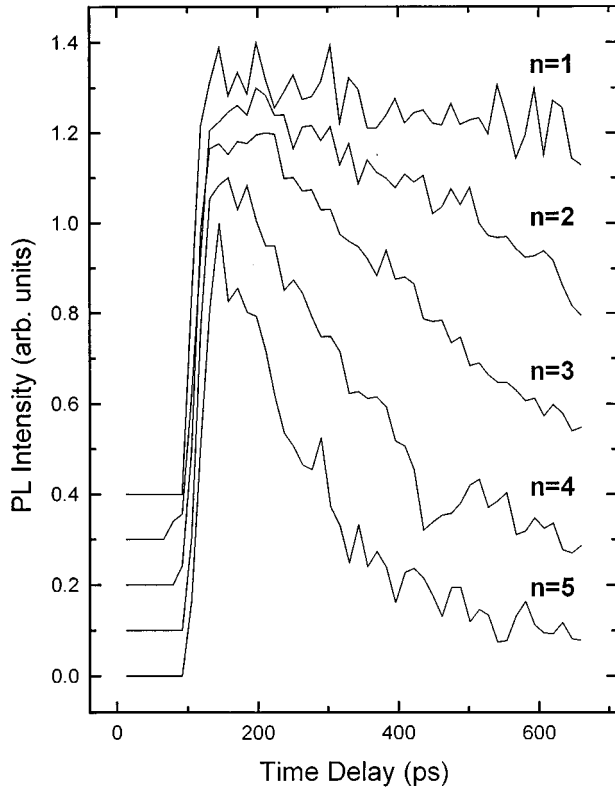


FIG. 4. Time decay of the various emission peaks spectra obtained by up-conversion measurements. The sample was excited with a YAG-pumped rhodamine 640 dye laser system producing 5-ps pulses and emitting at 630.0 nm. The average power at the sample was 1 mW, with a repetition rate of 76 MHz. Each trace was obtained at 4 K by monitoring the decay of one energy level (30-meV bandwidth for detection).

enter the dot via an excited state. This imposes that intersublevel relaxation times are much shorter than the excited-state radiative lifetimes, otherwise excited-state luminescence would be observed at low excitation power (phonon bottleneck effect), which is not seen in Fig. 2. The carrier population and therefore the PL intensity of a given excited state will be proportional to $\tau_{\text{ISL}}/(\tau_{\text{ISL}} + \tau_{\text{RAD}})$, where τ_{ISL} is the intersublevel relaxation time and τ_{RAD} is the radiative lifetime. This factor becomes negligible if $\tau_{\text{ISL}} \ll \tau_{\text{RAD}}$, and excited-state PL can be observed only if τ_{ISL} is comparable to τ_{RAD} . Since no excited-state emission is observed at low excitation intensities, the above condition must be satisfied for empty QD's, and we therefore interpret the longer decay

TABLE I. Decay times obtained by single-exponential fitting of the time-dependent curves.

Level	Peak position (eV)	Decay times (ns)		
		$P_{\text{exc}}=0.1$ mW	$P_{\text{exc}}=1.0$ mW	$P_{\text{exc}}=25$ mW
$n=1$	1.107	1.0	2.6	1.2
$n=2$	1.157	0.18	0.87	1.0
$n=3$	1.202	0.31	0.44	0.81
$n=4$	1.247		0.30	0.45
$n=5$	1.287		0.19	0.27

time, before the saturation caused by the upper state feeding process, as being the radiative lifetime (~ 1 ns). However, since excited-state PL can be observed at high excitation intensities, it is clear that intersublevel thermalization toward the lower levels is slowed due to the reduced number of available final states caused by the state-filling effect. As the intersublevel thermalization rate decreases and approaches the interband radiative recombination rate for a given excited-state transition, the spectra display a progressive saturation of the lower-energy transitions combined with the emergence of additional emission peaks originating from the upper excited states.

For the TRPL measurements all photoexcited carriers are created within 5 ps, i.e., before any radiative recombination can occur. At this point the QDs are empty and $\tau_{\text{ISL}} \ll \tau_{\text{RAD}}$, therefore capture times are fast compared to the radiative lifetimes, and state filling will occur for lower average excitation powers than in the cw case. This is observed in Fig. 2. Then, after the QD's are initially filled and neglecting non-radiative recombination,³⁸ the carriers can relax either by radiative recombination or intersublevel relaxation, except for carriers in the ground state which can decay by radiative recombination only. When a recombination event occurs, it creates an empty state. This empty state is eventually filled by a carrier coming from the upper levels, which in turn leaves an empty state in upper levels. This cascade stops when the highest occupied level loses a carrier which cannot be replaced. Thus the shorter intensity-dependent decay times of the upper excited states are a consequence of the state-filling effect. Also, the nonsingle exponential decay of lower-energy levels is caused by the constant supply of carriers coming from the upper states. For lower excitation intensity the initial occupation number $n(\omega)_0$ of all the states is lower, and the number of decay channels available for excited states becomes higher, and hence the shorter decay times observed. For such case of low excitation densities, some of the excited states may be initially empty. Under these conditions, the decay time of the highest occupied level is mainly determined by the intersublevel relaxation time. For 1.3-W/cm^2 excitation, the decay time of the $n=3$ level is 310 ps, and for a sequential picture in which carriers can only decay to the next lowest level, this time is an estimate of the $n=3-2$ intersublevel thermalization time. Note that since excited-state luminescence can still be observed, state-filling effects are present, and the empty dot intersublevel relaxation times are in fact much shorter than 310 ps. Inoshita and Sakaki³⁷ calculated that subnanosecond intersublevel relaxation times can be achieved for an energy spacing of one LO phonon with a tolerance of ~ 3 meV. For the sample studied in this paper, the combined electron and hole intersublevel spacings range from 40 to 50 meV. According to our calculations this corresponds to an electron spacing in the range of available phonons energies of 30 ± 3 and 36 ± 3 meV for the InAs-like and the GaAs-like LO-phonon energies respectively.^{4,5} These processes might therefore contribute to the fast thermalization toward the lower-energy states. In addition, Auger-like processes have been suggested to explain subnanosecond carrier relaxation in small QD's.^{8,2}

It is also interesting to note that the rise times for the various transitions at different excitation intensities are found to be virtually the same, and close to the temporal resolution

limit of our setup, namely, the 10–90 % rise times are 35 ± 5 ps. For a given energy level, this time is determined by the diffusion time to the dot region (τ_{rd}), the actual capture time from the top of the barrier to the discrete bound state considered (τ_c), and the intersublevel dynamics. If the rise time was dominated by the capture time (i.e., slow τ_c), one would expect τ_{rise} to be different for each level since Fig. 2 indicates that the lower levels will be filled first. Moreover, in this case the intersublevel dynamics would play a role, and depending if a particular level is beneath or above the initial Fermi level its rise time should change dramatically. Thus for slow τ_c one expects the rise times to be a function of energy level and excitation density. Equal rise times for all states at all intensities suggests that τ_{rise} is rather limited by carrier diffusion, which would imply that the actual capture times (τ_c) are much shorter than 35 ps. Future femtosecond resonant excitation experiments would help to clarify this fast capture dynamics.

In conclusion, excited-state PL was obtained in $\text{In}_{0.5}\text{Ga}_{0.5}\text{As}/\text{GaAs}$ self-assembled QD's, and up to five QD bound states were observed. Up-conversion was used to measure the decay time of the excited-state emission. The fast intersublevel thermalization of the bare excited states, which leads to a progressive state filling of the lower energy states, allowed the Fermi level to be raised by more than 200 meV due to the combined large intersublevel spacing and the low density of states. The decay time of each transition obtained under various excitation conditions has been used to evaluate the excited-state radiative lifetime, which is estimated to be ~ 1 ns (similar to the ground state lifetime), and the intersublevel thermalization time which is estimated to be at most a few hundred ps.

Part of this research was supported by NSF Science and Technology Center QUEST (DMR No. 91-20007), and by an AFOSR Grant (No. F49620-92-J-0124). One of us (S.R.) would also like to acknowledge NSERC for their additional support.

*Also at Department of Physics, University of Ottawa, Ottawa, Ontario, Canada K1N 6N5.

†Also at Department of Physics, Technical University of Wrocław, Wrocław 50-370, Poland.

‡Present address: Department of Electronic Materials Engineering, The Australian National University, Canberra, ACT, 0200, Australia.

§Present address: Department of Electrical Engineering, University of Notre Dame, Notre Dame, Indiana 46556-5602.

¹H. Benisty, C. M. Sotomayor-Torrès, and C. Weisbuch, *Phys. Rev. B* **44**, 10 945 (1991); H. Benisty, *ibid.* **51**, 13 281 (1995).

²U. Bockelmann and G. Bastard, *Phys. Rev. B* **42**, 8947 (1990); U. Bockelmann and T. Egeler, *ibid.* **46**, 15 574 (1992); U. Bockelmann, *ibid.* **48**, 17 637 (1993).

³K. Brunner, U. Bockelmann, G. Abstreiter, M. Walther, G. Böhm, G. Tränkle, and G. Weimann, *Phys. Rev. Lett.* **69**, 3216 (1992).

⁴S. Fafard, R. Leon, D. Leonard, J. L. Merz, and P. M. Petroff, *Phys. Rev. B* **52**, 5752 (1995).

⁵R. Heitz, M. Grundmann, N. N. Ledentsov, L. Eckey, M. Veit, D. Bimberg, V. M. Ustinov, A. Y. Egorov, A. E. Zhukov, P. S. Kop'ev, and Z. I. Alferov, *Appl. Phys. Lett.* **68**, 361 (1996).

⁶B. Bennett, B. V. Shanabrook, and R. Magno, *Appl. Phys. Lett.* **68**, 958 (1996).

⁷S. Raymond, S. Fafard, S. Charbonneau, R. Leon, D. Leonard, P. M. Petroff, and J. L. Merz, *Phys. Rev. B* **52**, 17 238 (1995).

⁸Al. L. Efros, V. A. Kharchenko, and M. Rosen, *Solid State Commun.* **93**, 281 (1995).

⁹D. Leonard, S. Fafard, K. Pond, Y. H. Zhang, J. L. Merz, and P. M. Petroff, *J. Vac. Sci. Technol. B* **12**, 2516 (1994).

¹⁰S. Fafard, R. Leon, D. Leonard, J. L. Merz, and P. M. Petroff, *Phys. Rev. B* **50**, 8086 (1994).

¹¹J.-Y. Marzin, J.-M. Gérard, A. Izraël, D. Barrier, and G. Bastard, *Phys. Rev. Lett.* **73**, 716 (1994).

¹²S. Fafard, D. Leonard, J. L. Merz, and P. M. Petroff, *Appl. Phys. Lett.* **65**, 1388 (1994).

¹³M. Grundmann, J. Christen, and N. N. Ledentsov *et al.*, *Phys. Rev. Lett.* **74**, 4043 (1995).

¹⁴R. Nötzel, J. Temmo, A. Kozen, T. Tamamura, T. Fukui, and H. Hasegawa, *Appl. Phys. Lett.* **66**, 2525 (1995).

¹⁵J. M. Moison, F. Houzay, F. Barthe, L. Leprince, E. André, and O. Vatel, *Appl. Phys. Lett.* **64**, 196 (1994).

¹⁶G. Wang, S. Fafard, D. Leonard, J. E. Bowers, J. L. Merz, and P. M. Petroff, *Appl. Phys. Lett.* **64**, 2815 (1994).

¹⁷S. Fafard, Z. Wasilewski, J. McCaffrey, S. Raymond, and S. Charbonneau, *Appl. Phys. Lett.* **68**, 991 (1996).

¹⁸A. Wojs, P. Hawrylak, S. Fafard, and L. Jacak, *Phys. Rev. B* (to be published).

¹⁹M. Grundmann, N. N. Ledentsov, O. Stier, D. Bimberg, V. M. Ustinov, P. S. Kop'ev, and Z. I. Alferov, *Appl. Phys. Lett.* **68**, 979 (1996).

²⁰H. Lipsanen, M. Sopanen, and J. Ahopelto, *Phys. Rev. B* **51**, 13 868 (1995).

²¹A. Zrenner, L. V. Butov, M. Hagan, G. Abstreiter, G. Böhm, and G. Weimann, *Phys. Rev. Lett.* **72**, 3382 (1994).

²²D. Gammon, E. S. Snow, and D. S. Katzer, *Appl. Phys. Lett.* **67**, 2391 (1995).

²³K. Brunner, G. Abstreiter, G. Böhm, G. Tränkle, and G. Weimann, *Phys. Rev. Lett.* **73**, 1138 (1994).

²⁴Q. Xie, A. Madhukar, P. Chen, and N. P. Kobayashi, *Phys. Rev. Lett.* **75**, 2542 (1995).

²⁵D. Leonard, K. Pond, and P. M. Petroff, *Phys. Rev. B* **50**, 11 687 (1994).

²⁶M. V. Marquezini, M. J. S. P. Brasil, J. A. Brum, P. Poole, S. Charbonneau, and M. C. Tamargo, *Surf. Sci.* (to be published).

²⁷H. Drexler, D. Leonard, W. Hansen, J. P. Kottaus, and P. M. Petroff, *Phys. Rev. Lett.* **73**, 2252 (1994).

²⁸P. D. Wang, J. L. Merz, S. Fafard, R. Leon, D. Leonard, G. Medeiros-Ribeiro, M. Oestreich, P. M. Petroff, K. Uchida, N. Miura, H. Ariyama, and H. Sakaki, *Phys. Rev. B* **53**, 16 458 (1996).

²⁹S. Raymond, P. Hawrylak, C. Gould, P. Zawadzki, A. Sachrajda, S. Charbonneau, S. Fafard, D. Leonard, P. M. Petroff, and J. L. Merz (unpublished).

³⁰D. Gammon, E. S. Snow, and D. S. Katzer, *Surf. Sci.* (to be published).

³¹S. Fafard, S. Raymond, G. Wang, R. Leon, D. Leonard, S. Charbonneau, J. L. Merz, P. M. Petroff, and J. E. Bowers, *Surf. Sci.* (to be published).

- ³²M. Grundman, O. Stier, and D. Bimberg, *Phys. Rev. B* **52**, 11 969 (1995).
- ³³R. Steffen, T. Koch, J. Oshinowo, F. Faller, and A. Forchel, *Surf. Sci.* (to be published).
- ³⁴J. Shah, *IEEE J. Quantum Electron.* **QE-24**, 276 (1988).
- ³⁵The PL spectra obtained in various regions of a 1.5×2 -mm² sample displayed no significant spectroscopic variations, indicating that this small piece contains no significant macroscopic inhomogeneities. This sample was cut in two parts which were then dedicated to the TEM and the optical studies presented here.
- ³⁶The possibility of segregated inhomogeneous alloy broadening remains, but it has never been observed and is therefore highly unlikely especially since it would not lead to intensity-dependent features.
- ³⁷T. Inoshita and H. Sakaki, *Phys. Rev. B* **46**, 7260 (1992).
- ³⁸Neglecting nonradiative recombination at 4 K is supported by the temperature dependence of the PL emission.